



Published in final edited form as:

Leukemia. 2017 April ; 31(4): 853–860. doi:10.1038/leu.2016.296.

The *LIN28B/let-7* axis is a novel therapeutic pathway in Multiple Myeloma

Salomon Manier^{1,2,3}, John T. Powers⁴, Antonio Sacco¹, Siobhan V. Glavey¹, Daisy Huynh¹, Michaela R. Reagan¹, Karma Z. Salem¹, Michele Moschetta¹, Jiantao Shi¹, Yuji Mishima¹, Catherine Roche-Lestienne³, Xavier Leleu², Aldo M. Roccaro¹, George Q. Daley⁴, and Irene M. Ghobrial¹

¹Department of Medical Oncology, Dana-Farber Cancer Institute, Harvard Medical School, Boston 02215 MA, USA

²Service des Maladies du Sang, CHRU Lille, 59000 Lille, France

³Jean-Pierre Aubert Research Centre, INSERM U1172, University Lille 2, 59000 Lille, France

⁴Division of Pediatric Hematology/Oncology, Children's Hospital, Harvard Medical School, Boston 02215 MA, USA

Abstract

MYC is a major oncogenic driver of Multiple Myeloma (MM) and yet almost no therapeutic agents exist that target *MYC* in MM. Here we report that the *let-7* biogenesis inhibitor *LIN28B* correlates with *MYC* expression in MM and is associated with adverse outcome. We also demonstrate that the *LIN28B/let-7* axis modulates the expression of *MYC*, itself a *let-7* target. Further, perturbation of the axis regulates the proliferation of MM cells *in vivo* in a xenograft tumor model. RNA sequencing and gene set enrichment analyses of CRISPR-engineered cells further suggest that the *LIN28B/let-7* axis regulates *MYC* and cell cycle pathways in MM. We provide proof-of-principle for therapeutic regulation of *MYC* through *let-7* with an LNA-GapmeR containing a *let-7b* mimic *in vivo*, demonstrating that high levels of *let-7* expression repress tumor growth by regulating *MYC* expression. These findings reveal a novel mechanism of therapeutic targeting of *MYC* through the *LIN28B/let-7* axis in MM that may impact other *MYC* dependent cancers as well.

Users may view, print, copy, and download text and data-mine the content in such documents, for the purposes of academic research, subject always to the full Conditions of use: http://www.nature.com/authors/editorial_policies/license.html#terms

Corresponding author: Irene M. Ghobrial, Medical Oncology, Dana-Farber Cancer Institute, HIM 237, 77 Ave Louis Pasteur, Boston, Massachusetts 02115, USA. Phone: 617.632.4198; Fax: 617.632.4862; irene_ghobrial@dfci.harvard.edu.

Conflicts of Interest Disclosure

We declare that we have no conflicts of interest.

Authors' Contributions

S.M., J.T.P., G.Q.D., I.M.G designed research; S.M., A.S., S.V.G, D.H., M.R.R., Y.M. performed *in vitro* research; S.M., K.S., M.M. performed *in vivo* research; J.S. processed RNA-sequencing data; S.M., J.T.P., C.R-L., X.L, A.M.R., G.Q.D., I.M.G analyzed data; S.M., J.T.P., S.V.G, G.Q.D., I.M.G wrote the paper.

RNA-seq data have been deposited to the Gene Expression Omnibus (<http://www.ncbi.nlm.nih.gov/geo/>) under accession numbers GSE71100.

Introduction

Multiple myeloma (MM), a tumor originating from plasma cells in the bone marrow (BM), has an annual incidence of 6.3 new cases per 100,000 individuals¹. Despite the major advances in therapy for MM, it remains incurable and there are no targeted therapies for MM, in part due to the lack of therapies that target specific oncogenes involved in the pathogenesis of the disease. Genomic events such as chromosomal translocations, copy number variation, somatic mutations, and epigenetic modifications all contribute to gene deregulation of specific oncogenes or tumor suppressors during MM tumorigenesis². Among those, *MYC* plays a central role in the progression of the disease. Approximately two thirds of newly diagnosed patients harbor *MYC* activation, which correlates with adverse clinical outcome³. *MYC* activation is commonly driven by translocation or copy number gain of chromosome 8q24, which contains the *MYC* locus^{4,5}. Despite the dominant role of *MYC* in MM, there are very few therapeutic options targeting *MYC*. Previous studies have attempted to target *MYC* by using a bromodomain inhibitor to target BET proteins, which regulate *MYC*^{6,7}.

The *let-7* miRNA was originally discovered in *C. elegans* as a regulator of developmental timing and cell proliferation⁸. *Let-7* expression increases as cells become more differentiated. In humans, *let-7* miRNAs comprise a family of 12 members distributed over 8 genomic loci⁹ that are often repressed in cancer¹⁰. *Let-7* miRNAs function as a tumor suppressor through regulation of key oncogenes, including *MYC* and *RAS*, by binding specific sites in the mRNA 3'-UTRs and inhibiting translation of these targets^{11,12}. Low expression of *let-7* family members is associated with poor prognosis in several cancer types^{13,14}.

In humans, *let-7g* and *let-7i* are located individually on chromosomes 3 and 12 respectively. The remaining *let-7* family members are distributed among six miRNA clusters at genetically distinct loci. The *let-7a2* and *let-7c* clusters are involved in hematopoietic stem and progenitor cell (HSPC) homeostasis by regulating the balance between TGF β and Wnt signaling¹⁵, whereas the *let-7e* cluster is highly expressed in HSPC and confers hematopoietic phenotypes¹⁶. However, the exact role of the various *let-7* family members in mammalian development has not yet been fully elucidated^{17,18}, in large part because it is technically difficult to knock out multiple *let-7* family members in the same individual cell. Moreover, these multiple *let-7* family members are likely to have functionally similar roles.

LIN28B is an RNA-binding protein highly expressed in stem cells and developing tissues where it impairs the processing of *let-7* precursors into mature, functional miRNAs¹⁹. Overexpression of *LIN28B* has been reported in several cancers²⁰ and is associated with advanced disease and poor outcome in ovarian¹⁴, breast²¹, colon²², hepatocellular carcinoma^{23,24} and neuroblastoma^{25,26}. Transgenic *LIN28B* has been shown to induce multiple tumor types in mice including liver, Wilms, colon, and neuroblastoma, all of which solidify its oncogenic role^{24,25,27,28}. *LIN28B* has also been reported to act through a *let-7*-independent manner, especially via regulation of *IGF2*²⁴.

While the *LIN28B/let-7* axis has been implicated in the regulation of *MYC* in different tumor types²⁰, its potential as a therapeutic target has not yet been explored, specifically in blood cancers. In this study, we define the mechanistic activity of the *LIN28/let-7* axis in clonal plasma cells and establish a potential therapeutic role of this pathway in targeting *MYC* in MM, which could lead to significant therapeutic advances in MM and other cancers.

Methods

Cell and primary cells

The MM cell lines MM.1S and RPMI8226 were purchased from ATCC; KMS12BM and MOLP-8 were purchased from DSMZ and KMM-1 was purchased from JCRB Cell Bank. The MM.1S GFP⁺Luc⁺ cell line was generated by retroviral transduction with the pGC-GFP/Luc vector (gift of A. Kung, Dana-Farber Cancer Institute). Cells were authenticated by short tandem repeat DNA profiling. Primary samples were obtained from bone marrow aspiration from both MM patients and healthy controls. Plasma cells were isolated using CD138⁺ microbead selection (Miltenyi Biotec®, Auburn, CA). All patients were diagnosed with active MM at diagnosis or at relapse, based on criteria of the International Myeloma Working Group²⁹. Informed consent was obtained from all patients and healthy volunteers in accordance with the Declaration of Helsinki protocol.

Lentivirus-mediated shRNA silencing

LIN28B shRNA in lentiviral plasmid (TRCN0000122191 and TRCN0000122599) and control shRNA (SHC216V) were purchased from Sigma-Aldrich. For viral production, 293T cells were transfected with lentiviral gag/pol, VSV-G, and the lentiviral plasmid, at a ratio of 1:0.4:1, using Lipofectamine 2000. Viral particles were harvested after 24hrs and 48hrs. Two milliliters of viral supernatant were used to infect 1,000,000 cells in the presence of Polybrene (8 ng/μL). Infected cells were selected on Puromycin antibiotic before subsequent analysis.

Lentivirus-mediated CRISPR silencing

LentiCRISPRv2 (Addgene plasmid #52961) and lentiCRISPR:EGFPsgRNA-1 (#51760) were gifts from Feng Zhang³⁰. *LIN28B* sgRNA were designed using the MIT Optimized CRISPR design tool. Sequences of sgRNA were: 5'-CATCGACTGGAATATCCAA G-3' for sg*LIN28B*#1 and 5'-CAGAGCAAACATTCATGGA-3' for sg*LIN28B*#2. Human U6 (hU6) primer 5'-GAGGGCCTATTTCCCATGATT-3' was used for validation by Sanger sequencing after cloning. Lentivirus production was processed as above for shRNA lentiviral production.

miRNA mimic transfection

Cell lines were transfected with hsa-let-7b mimic or with a control probe (mirVana miRNA mimic, Life Technology) at final concentration of 40 nM, using Lipofectamine 2000 according to manufacturer's instructions (Invitrogen). Culture medium was changed to regular medium 24 hours after transfection and cells were used for functional assays at 48 hours. For the rescue experiment, MOLP-8 sgGFP or sg*LIN28B*#1 were transfected with a

control probe or a mix of anti-*let-7a*, *b*, *d*, and *g* (mirVana anti-miRNA, Life Technology) at a final concentration of 40 nM, using X-tremeGENE 9 according to manufacturer's instructions (Roche, Life Science).

Quantitative reverse transcription PCR

Mature miRNA and mRNA expression were analyzed by qRT-PCR using SYBR green dye on an Applied Biosystems AB7500 Real Time PCR System. All PCR reactions were run in triplicate. Ct values were normalized on RNU6B and 18S, respectively, and relative changes were calculated using the 2^{-Ct} . The following primer sequences were used: *LIN28B*-F: 5'-GCCCTTGGATATTCCAGTC-3'; *LIN28B*-R: 5'-TGACTCAAGGCCTTTGGAAG-3'; *MYC*-F: 5'-TCGGTCCTCGGATTCTCTGCTCT-3'; *MYC*-R: 5'-GCCTCCAGCAGAAGGTGATCCA-3'; *KRAS*-F: 5'-TGTGTCTCATATCAGGTTGACGA-3'; *KRAS*-R: 5'-CAAGAGTCGAGTGTGGTCTCA-3'; *CCND1*-F: 5'-TCTACACCGACAACCTCCATCCG-3'; *CCND1*-R: 5'-TCTGGCATTGAGAGGAAGTG-3'; *DICER1*-F: 5'-CTCCTACCACTACAATACTATCACT-3'; *DICER1*-R: 5'-GGTCTTCATAAAGGTGCTTGGT-3'; *E2F6*-F: 5'-GCGGAGAGTGTATGACATCACC-3'; *E2F6*-R: 5'-GTCAGAAAGTTCCTCCTGTAGCT-3'; *HMGA1*-F: 5'-GAAGTGCCAACACCTAAGAGACC-3'; *HMGA1*-R: 5'-GGTTTCCTTCCTGGAGTTGTGG-3'; *pri-let-7d*-F: 5'-GCCAAGTAGAAGACCAGCAAG-3'; *pri-let-7d*-R: 5'-CAAGGAAACAGTTATCGGTG-3'; *pri-let-7g*-F: 5'-GTTCCCTCCAGCGCTCCGTT-3'; *pri-let-7g*-R: 5'-CCATTACCTGGTTTCCCAGAGA-3'. Sequences for full mature *let-7* miRNA were used to design *let-7* forward primers, in combination with universal 3' miRNA reverse primer.

Immunoblotting

Whole-cell lysates were subjected to SDS-PAGE, and transferred to polyvinylidene fluoride (PVDF) membrane (Bio-Rad Laboratories). For immunoblotting we used antibodies against *LIN28B* (Cell signaling #4196S), *c-MYC* (Cell signaling #9402S) and GAPDH (Cell signaling #2118S).

Proliferation assay

Proliferation rates were measured by DNA synthesis, using [³H]-thymidine uptake (Perkin Elmer, Boston, MA) as described³¹.

RNA-sequencing

RNA was extracted using Qiagen RNeasy Kit. Whole RNA (500ng) was subject to library preparation with NEBNext Ultra RNA Library prep for Illumina kit (BioLabs). A single unique index was assigned to each sample. Quality control of the libraries was evaluated by Bioanalyzer analysis with High Sensitivity chips (Agilent). Libraries were quantified by qPCR (Kapa assay) and multiplex before sequencing on a HiSeq 2000 (2×50bp paired-end reads) at the Biopolymers Facility of Harvard Medical School. Cutadapt was used to trim

adapters; trimmed reads were aligned to Human reference genome (GRCh37) with tophat2; and read counts for each gene was calculated by HT-seq. RNA-seq data have been deposited to the Gene Expression Omnibus (<http://www.ncbi.nlm.nih.gov/geo/>) under accession numbers GSE71100.

In vivo studies

SCID/bg mice (n=5/group) used for xenograft experiments were injected subcutaneously with MOLP-8 cells that were infected with either a *LIN28B* shRNA, or a control shRNA. Tumor volume (measured by caliper) were calculated by the formula: length \times width² \times 0.52³². To evaluate the effect of *let-7* LNA-GapmeR (containing the sequence 5'-AGGTAGTAGGTTGTGT-3'), SCID/bg mice (n=5/group) were i.v. injected with 5 \times 10⁶ MM.1S GFP⁺Luc⁺ cells on day 0; followed by i.p. injections of *let-7* (20 mg/kg) or control LNA-GapmeR 2 times a week starting on day 2. Tumor growth was evaluated by bioluminescence imaging (BLI) and mice were followed for survival.

Results

Deregulation of *LIN28B/Let-7* axis in MM

We first sought to determine whether *LIN28B* is deregulated in MM, and therefore analyzed two independent publicly available gene expression profiling datasets containing plasma cells from patients with newly diagnosed MM and healthy control donors. These included GSE24080 and GSE2658, containing 22 normal donor plasma cell samples and 559 plasma cell samples from patients with newly diagnosed patients - both from UAMS - and GSE16558, with 5 normal donor plasma cells and 65 plasma cell samples from patients with newly diagnosed MM. We identified a significant overexpression of *LIN28B* in MM cells compared to normal plasma cells in both datasets (Fig. 1a). We next sought to determine the prognostic relevance of *LIN28B* in the survival of patients with MM. We performed Kaplan Meier analysis on a cohort of 542 patients treated with Total Therapy 2 (GSE2658), and observed that high expression of *LIN28B* was associated with significantly worse overall survival, (p=0.0075) (Fig. 1b).

Therefore, we explored whether targeting the *LIN28B/let-7 axis* would have a therapeutically relevant role in MM and silenced *LIN28B* using two lentiviral short hairpins (shRNA) constructs that target the mRNA coding sequence in several *LIN28B*-expressing MM cell lines: MOLP-8, KMS12BM, RPMI8226 and KMM-1. The shRNAs caused degradation of *LIN28B* mRNA in all cell lines (Fig. 1c). Moreover, pri-*let-7* RNA was not modified as shown for pri-*let-7g*, consistent with the post-transcriptional regulation of *let-7* by *LIN28B* (Supplemental Fig. 1a).

***LIN28B* regulates *let-7* and *MYC* in MM**

Consistent with the role of *LIN28B* in regulating *let-7* expression, we observed de-repression of *let-7* family members in cells with *LIN28B* knockdown compared to non-targeting control (Fig. 2a). We next analyzed the downstream targets of *LIN28B/let-7* and found a decreased protein expression of *MYC* in *LIN28B*-silenced cells in several MM cell lines (Fig. 2b). Moreover, knockdown of *LIN28B* significantly impaired the proliferation of

these cell lines tested (Fig. 2c). Consistent with these observations, we identified, through gene set enrichment analysis (GSEA), an enrichment of *let-7* target genes in MM patient samples who displayed a high level of *LIN28B* expression in two independent datasets (GSE2658 and MMRC dataset), suggesting that *LIN28B* represses *let-7* and indirectly enriches *let-7* target expression (Fig. 3a).

In addition, among *let-7* target genes, *MYC* expression significantly correlated with *LIN28B* expression level in two independent datasets (GSE16558 and GSE2658). As shown in Supplemental Fig. 1b, a strong correlation existed between *LIN28B* and *MYC* in MM tumor cells from patient samples in GSE16558 and in total therapy 2 GSE2658, $p < 0.028$ and $p < 0.001$, respectively.

To validate whether MM cells are dependent on *LIN28B* for growth, we examined tumor growth of MOLP-8 cell line with a *LIN28B* specific hairpin or non-targeting control in a xenograft mouse model using SCID/bg mice. Tumor growth was significantly lower in mice injected subcutaneously with *LIN28B* knockdown compared to scrambled control (Fig. 3b), resulting in a significant prolongation of survival in the experimental group, $p = 0.0045$ (Fig. 3c). In addition, *MYC* expression was significantly reduced in cells obtained ex-vivo from mice injected with *LIN28B* knockdown compared to scrambled control (Supplemental Fig. 1c).

Together, these data suggest a deregulation of *LIN28B/let-7* axis in a proportion of patients with MM and can function as a novel therapeutic target of *MYC* regulation in MM.

MYC* and cell cycle pathways are highly enriched in cells with high expression of *LIN28B

To control for possible off-target effect of shRNAs and for incomplete *LIN28B* knockdown mitigating the observed phenotype, we next used CRISPR/Cas9 technology to knock-out (KO) *LIN28B* in the MOLP-8 cell line. Single guide RNAs (sgRNA) targeting exons 2 and 3 of *LIN28B* were used (Supplemental Fig. 2a). Significant decrease in *LIN28B* protein levels were observed, indicating high frequency *LIN28B* KO in the cell population. *MYC* protein level were similarly decreased (Fig. 4a). Moreover, *LIN28B* KO resulted in de-repression of *let-7*, which was consistent with the shRNA experiment (Fig. 4b). Moreover, *LIN28B* KO led to the reduced proliferation by thymidine uptake assay (Fig. 4c).

For further characterization of the *LIN28B/let-7* axis in MM, we performed RNA-sequencing of the *LIN28B* CRISPR-KO cells and *GFP* sgRNA control cells in triplicate. *LIN28B* was confirmed to be the most significantly down-regulated gene in *LIN28B*-silenced cells (Fig. 5a), confirming efficient knock-out. We then queried the top 150 down regulated genes in *LIN28B* KO cells against the MSigDB 'H' hallmark, 'c2' canonical pathways and 'c3' transcription factor target gene sets. The 10 most enriched gene sets were present in *E2F* cell cycle pathway regulation (Fig. 5b). Of note, *E2F2*, a *let-7* target gene, was one of the most down-regulated genes in *LIN28B* KO cells. Moreover, we found a significant enrichment of *let-7* target genes in control compared to *LIN28B* KO cells (Fig. 6a). Using an unsupervised GSEA analysis of the whole data set against the MSigDB 'H' hallmark gene sets, we found that *MYC* pathway gene set was in the top 5 genes sets, which further suggests that the *LIN28B/let-7* axis regulates *MYC* in MM. Moreover, significant

enrichment of *MYC* pathway in control cells was also validated using several *MYC* pathway gene sets (Fig. 6b). These results support a model where *LIN28B* represses *let-7*, thereby enriching *let-7* targets such as *E2F2* and *MYC* in MM.

Given that *LIN28B* has been reported to act both in a *let-7*-dependent and independent manner³³, we next asked whether the functional role of *LIN28B* is mediated via *let-7* in MM. We thus performed a rescue experiment by transfection of a *let-7* inhibitor into *LIN28B*-KO MOLP-8 cells. We observed a significant decrease of *let-7* family members in *LIN28B* KO cells plus the anti-*let-7* (Fig. 6c). *Let-7* inhibition also significantly rescued cell proliferation (Supplemental Fig. 2b), indicating that *let-7* is likely the main target of direct regulation by *LIN28B*, in *let-7* dependent manner in MM.

Deregulation of *let-7* in MM

Given that we demonstrated that *LIN28B* regulates MM proliferation through *let-7*, we sought to define the direct role of *let-7* in MM. We first assessed the expression level of *let-7* family members in primary bone marrow MM CD138⁺ cells compared to healthy control CD138⁺ bone marrow plasma cells by qRT-PCR. *Let-7* miRNAs were lower in plasma cells from six patients with relapsed MM and in four MM cell lines, as compared to plasma cells from three healthy donors (Fig. 7a). To determine whether *let-7* directly regulates *MYC* in MM, we transfected a *let-7b* mimic into MM.1S cells (Supplemental Fig. 3a) and observed a reduction of cell proliferation (Fig. 7b) as well as a decrease level of *MYC* protein (Supplemental Fig. 3b). To validate these findings in patient samples, we assessed the correlation between *let-7* and *MYC* expressions in publicly available gene expression profiling with matched miRNA array from MM patients (GSE16558). We found a significant inverse correlation between expression of *let-7b* and *g* and the expression level of *MYC* in a cohort of 60 patients (Fig. 7c). These data support the idea that *LIN28B* acts in a *let-7*-dependent manner in MM and suggest that low expression levels of *let-7* in MM patients contributes to *MYC* dysregulation and tumor proliferation.

Let-7 as a potential therapeutic target that regulates *MYC* in MM

We next sought to confirm the importance of *let-7* in MM *in vivo* and to assess whether *let-7* could serve as a therapeutic strategy to directly target *MYC* in MM. We therefore developed a *let-7* Locked Nucleic Acid (LNA)-GapmeR mimic, which was designed based on the seed region of *let-7* miRNAs to efficiently mark *let-7* target genes for degradation by RNase H. We first tested the ability of the *let-7* LNA-GapmeR to decrease *let-7* target genes *in vitro*. MM.1S cell line was cultured in presence of a control probe or three different concentrations of *let-7* LNA GapmeR (10nM, 100nM and 1uM). By qRT-PCR we observed a consistent decrease of *MYC*, *KRAS*, *CCND1*, *E2F6*, *DICER1* and *HMGA1* expression levels in parallel to increased concentration of the GapmeR (Supplemental Fig. 4a). We next tested the *let-7* LNA-GapmeR *in vivo* in a xenograft mouse model. SCID/bg mice were injected with 5×10^6 MM.1S GFP⁺Luc⁺ cells intravenously, followed by intraperitoneal (i.p.) injections of *let-7* LNA-GapmeR two times a week. The treatment was well tolerated and did not induce obvious toxicity or weight loss. The tumor growth was evaluated by BLI, and was significantly reduced in the group of mice that received *let-7* LNA-GapmeR as compared to the control group, $p=0.018$ (Fig. 8a and Supplemental Fig. 4b). This was

associated with consequent significant survival benefit, $p=0.026$ (Fig. 8b). *Ex-vivo*, MM cells were analyzed for *MYC* expression, confirming the repression of *MYC* in the *let-7* LNA-GapmeR group (Fig. 8c). This experiment provides proof of principle that *let-7* could represent a new therapeutic approach targeting *MYC* in MM.

Discussion

In this study, we describe the role of the *LIN28B/let-7* axis in MM and identify *let-7* as a potential new therapeutic approach for targeting *MYC*. High expression of *LIN28B* in MM is associated with both adverse outcomes and *MYC* overexpression. *LIN28B* represses *let-7* expression in MM cells, resulting in deregulation of *MYC* protein and cell proliferation *in vitro* and *in vivo*. A pathway enrichment analysis in *LIN28B* KO cells reveals the importance of the *MYC* and *E2F* cell cycle pathways within the *LIN28B/let-7* axis. Moreover, *LIN28B*-induced proliferation and *MYC* deregulation is *let-7* dependent. The tumor growth impairment *in vivo* by administration of a *let-7b* based LNA-GapmeR provides proof of principle for a new therapeutic option to target *MYC* in MM (Supplemental Fig. 5).

Let-7 miRNAs have been described as tumor suppressor in several cancers, by targeting major oncogenic pathways⁹. Copy number loss^{34–36} or epigenetic silencing³⁷ of individual *let-7* family members has been reported in some cancers. In MM, several *let-7* genes are located in frequently deleted regions, such as *let-7g* at 3p21, *let-7i* at 12q14, or *let-7a-2* at 11q24. These copy number aberrations might participate in deregulation of the *LIN28B/let-7* axis in MM. Here, we have described a mechanism of regulation of *let-7* miRNAs in MM involving *LIN28B*, which inhibits *let-7* miRNAs, resulting in deregulation of the *MYC* and *E2F* cell cycle pathways. Although *LIN28B* has been reported in liver cancer to act through both *let-7*-dependent and *let-7*-independent manners²⁴, our findings suggest the predominance of a *let-7*-dependent mechanism in MM.

LIN28B is located in the 6q21 cytogenetic band, which is amplified in some cases of neuroblastoma, resulting in *LIN28B* overexpression²⁵. In MM, previously published CGH array did not find amplification at 6q21 locus³⁸. The increased expression of *LIN28B* might therefore result from epigenetic changes such as altered methylation or histone modification or deregulation of upstream processes. *MiR-125b* was reported to inhibit *LIN28B* in embryonic stem cells as well as in some case of cancers^{25, 39, 40}. Interestingly, *miR-125b* is located in 11q23, which is frequently deleted in MM. Of note, *let-7* miRNAs themselves have also been reported to regulate *LIN28B* expression, in a feedback loop manner⁴¹. Moreover, a recent report suggests that inactivation of *DIS3* increases *LIN28B* expression in MM⁴², by impairing its mRNA degradation. *DIS3* is an exosome endoribonuclease involved in the turnover and degradation of mRNA in the cytoplasm. Strikingly, *DIS3* is one of the most frequently mutated genes in MM^{43, 44}, further suggesting a central role for *LIN28B/let-7* axis in MM.

Despite key roles for *MYC* in MM, there are very few therapeutic options targeting *MYC*. Previous studies attempted to target *MYC* by using a bromodomain inhibitor to target BET proteins, which regulate *MYC*^{6, 7}. The clinical impact of these inhibitors is being elucidated

in early phase clinical trials with some potentially promising results in hematological malignancies. Our findings provide proof of principle that therapeutic use of *let-7* can allow the repression of multiple oncogenes concurrently in MM. We show that *in vivo* use of *let-7* effectively regulates *MYC*, which is an essential regulator of tumor progression in MM and other cancers. Our findings indicate the importance of *let-7* regulation in MM and suggest that *let-7* may be an effective therapeutic option that can directly target *MYC* in MM.

Supplementary Material

Refer to Web version on PubMed Central for supplementary material.

Acknowledgments

S.M. was supported by a grant from ARC Foundation. This work was supported by a grant from the National Cancer Institute (R01CA154648).

References

1. Howlader N, Noone AM, Yu M, Cronin KA. Use of imputed population-based cancer registry data as a method of accounting for missing information: application to estrogen receptor status for breast cancer. *Am J Epidemiol*. 2012 Aug 15; 176(4):347–356. [PubMed: 22842721]
2. Morgan GJ, Walker BA, Davies FE. The genetic architecture of multiple myeloma. *Nat Rev Cancer*. 2012 May; 12(5):335–348. [PubMed: 22495321]
3. Chng WJ, Huang GF, Chung TH, Ng SB, Gonzalez-Paz N, Troska-Price T, et al. Clinical and biological implications of MYC activation: a common difference between MGUS and newly diagnosed multiple myeloma. *Leukemia*. 2011 Jun; 25(6):1026–1035. [PubMed: 21468039]
4. Walker BA, Wardell CP, Murison A, Boyle EM, Begum DB, Dahir NM, et al. APOBEC family mutational signatures are associated with poor prognosis translocations in multiple myeloma. *Nature communications*. 2015; 6:6997.
5. Affer M, Chesi M, Chen WD, Keats JJ, Demchenko YN, Tamizhmani K, et al. Promiscuous MYC locus rearrangements hijack enhancers but mostly super-enhancers to dysregulate MYC expression in multiple myeloma. *Leukemia*. 2014 Aug; 28(8):1725–1735. [PubMed: 24518206]
6. Mertz JA, Conery AR, Bryant BM, Sandy P, Balasubramanian S, Mele DA, et al. Targeting MYC dependence in cancer by inhibiting BET bromodomains. *Proc Natl Acad Sci U S A*. 2011 Oct 4; 108(40):16669–16674. [PubMed: 21949397]
7. Delmore JE, Issa GC, Lemieux ME, Rahl PB, Shi J, Jacobs HM, et al. BET bromodomain inhibition as a therapeutic strategy to target c-Myc. *Cell*. 2011 Sep 16; 146(6):904–917. [PubMed: 21889194]
8. Reinhart BJ, Slack FJ, Basson M, Pasquinelli AE, Bettinger JC, Rougvie AE, et al. The 21-nucleotide *let-7* RNA regulates developmental timing in *Caenorhabditis elegans*. *Nature*. 2000 Feb 24; 403(6772):901–906. [PubMed: 10706289]
9. Roush S, Slack FJ. The *let-7* family of microRNAs. *Trends Cell Biol*. 2008 Oct; 18(10):505–516. [PubMed: 18774294]
10. Lu J, Getz G, Miska EA, Alvarez-Saavedra E, Lamb J, Peck D, et al. MicroRNA expression profiles classify human cancers. *Nature*. 2005 Jun 9; 435(7043):834–838. [PubMed: 15944708]
11. Sampson VB, Rong NH, Han J, Yang Q, Aris V, Soteropoulos P, et al. MicroRNA *let-7a* down-regulates MYC and reverts MYC-induced growth in Burkitt lymphoma cells. *Cancer Res*. 2007 Oct 15; 67(20):9762–9770. [PubMed: 17942906]
12. Johnson SM, Grosshans H, Shingara J, Byrom M, Jarvis R, Cheng A, et al. RAS is regulated by the *let-7* microRNA family. *Cell*. 2005 Mar 11; 120(5):635–647. [PubMed: 15766527]
13. Takamizawa J, Konishi H, Yanagisawa K, Tomida S, Osada H, Endoh H, et al. Reduced expression of the *let-7* microRNAs in human lung cancers in association with shortened postoperative survival. *Cancer research*. 2004 Jun 1; 64(11):3753–3756. [PubMed: 15172979]

14. Shell S, Park SM, Radjabi AR, Schickel R, Kistner EO, Jewell DA, et al. Let-7 expression defines two differentiation stages of cancer. *Proc Natl Acad Sci U S A*. 2007 Jul 3; 104(27):11400–11405. [PubMed: 17600087]
15. Emmrich S, Rasche M, Schoning J, Reimer C, Keihani S, Maroz A, et al. miR-99a/100~125b tricistrons regulate hematopoietic stem and progenitor cell homeostasis by shifting the balance between TGFbeta and Wnt signaling. *Genes Dev*. 2014 Apr 15; 28(8):858–874. [PubMed: 24736844]
16. Gerrits A, Walasek MA, Olthof S, Weersing E, Ritsema M, Zwart E, et al. Genetic screen identifies microRNA cluster 99b/let-7e/125a as a regulator of primitive hematopoietic cells. *Blood*. 2012 Jan 12; 119(2):377–387. [PubMed: 22123844]
17. Schulman BR, Esquela-Kerscher A, Slack FJ. Reciprocal expression of lin-41 and the microRNAs let-7 and mir-125 during mouse embryogenesis. *Dev Dyn*. 2005 Dec; 234(4):1046–1054. [PubMed: 16247770]
18. Wulczyn FG, Smirnova L, Rybak A, Brandt C, Kwidzinski E, Ninnemann O, et al. Post-transcriptional regulation of the let-7 microRNA during neural cell specification. *FASEB J*. 2007 Feb; 21(2):415–426. [PubMed: 17167072]
19. Viswanathan SR, Daley GQ, Gregory RI. Selective blockade of microRNA processing by Lin28. *Science*. 2008 Apr 4; 320(5872):97–100. [PubMed: 18292307]
20. Viswanathan SR, Powers JT, Einhorn W, Hoshida Y, Ng TL, Toffanin S, et al. Lin28 promotes transformation and is associated with advanced human malignancies. *Nature genetics*. 2009 Jul; 41(7):843–848. [PubMed: 19483683]
21. Feng C, Neumeister V, Ma W, Xu J, Lu L, Bordeaux J, et al. Lin28 regulates HER2 and promotes malignancy through multiple mechanisms. *Cell cycle*. 2012 Jul 1; 11(13):2486–2494. [PubMed: 22713243]
22. King CE, Cuatrecasas M, Castells A, Sepulveda AR, Lee JS, Rustgi AK. LIN28B promotes colon cancer progression and metastasis. *Cancer research*. 2011 Jun 15; 71(12):4260–4268. [PubMed: 21512136]
23. Guo Y, Chen Y, Ito H, Watanabe A, Ge X, Kodama T, et al. Identification and characterization of lin-28 homolog B (LIN28B) in human hepatocellular carcinoma. *Gene*. 2006 Dec 15; 384:51–61. [PubMed: 16971064]
24. Nguyen LH, Robinton DA, Seligson MT, Wu L, Li L, Rakheja D, et al. Lin28b is sufficient to drive liver cancer and necessary for its maintenance in murine models. *Cancer Cell*. 2014 Aug 11; 26(2):248–261. [PubMed: 25117712]
25. Molenaar JJ, Domingo-Fernandez R, Ebus ME, Lindner S, Koster J, Drabek K, et al. LIN28B induces neuroblastoma and enhances MYCN levels via let-7 suppression. *Nature genetics*. 2012 Nov; 44(11):1199–1206. [PubMed: 23042116]
26. Diskin SJ, Capasso M, Schnepf RW, Cole KA, Attiyeh EF, Hou C, et al. Common variation at 6q16 within HACE1 and LIN28B influences susceptibility to neuroblastoma. *Nature genetics*. 2012 Oct; 44(10):1126–1130. [PubMed: 22941191]
27. Urbach A, Yermalovich A, Zhang J, Spina CS, Zhu H, Perez-Atayde AR, et al. Lin28 sustains early renal progenitors and induces Wilms tumor. *Genes Dev*. 2014 May 1; 28(9):971–982. [PubMed: 24732380]
28. Tu HC, Schwitalla S, Qian Z, LaPier GS, Yermalovich A, Ku YC, et al. LIN28 cooperates with WNT signaling to drive invasive intestinal and colorectal adenocarcinoma in mice and humans. *Genes Dev*. 2015 May 15; 29(10):1074–1086. [PubMed: 25956904]
29. International Myeloma Working G. Criteria for the classification of monoclonal gammopathies, multiple myeloma and related disorders: a report of the International Myeloma Working Group. *British journal of haematology*. 2003 Jun; 121(5):749–757. [PubMed: 12780789]
30. Shalem O, Sanjana NE, Hartenian E, Shi X, Scott DA, Mikkelsen TS, et al. Genome-scale CRISPR-Cas9 knockout screening in human cells. *Science*. 2014 Jan 3; 343(6166):84–87. [PubMed: 24336571]
31. Leleu X, Jia X, Runnels J, Ngo HT, Moreau AS, Farag M, et al. The Akt pathway regulates survival and homing in Waldenstrom macroglobulinemia. *Blood*. 2007 Dec 15; 110(13):4417–4426. [PubMed: 17761832]

32. Tomayko MM, Reynolds CP. Determination of subcutaneous tumor size in athymic (nude) mice. *Cancer chemotherapy and pharmacology*. 1989; 24(3):148–154. [PubMed: 2544306]
33. Shyh-Chang N, Daley GQ. Lin28: primal regulator of growth and metabolism in stem cells. *Cell Stem Cell*. 2013 Apr 4; 12(4):395–406. [PubMed: 23561442]
34. Zhang L, Volinia S, Bonome T, Calin GA, Greshock J, Yang N, et al. Genomic and epigenetic alterations deregulate microRNA expression in human epithelial ovarian cancer. *Proc Natl Acad Sci U S A*. 2008 May 13; 105(19):7004–7009. [PubMed: 18458333]
35. Nagayama K, Kohno T, Sato M, Arai Y, Minna JD, Yokota J. Homozygous deletion scanning of the lung cancer genome at a 100-kb resolution. *Genes, chromosomes & cancer*. 2007 Nov; 46(11):1000–1010. [PubMed: 17674361]
36. Yamada H, Yanagisawa K, Tokumaru S, Taguchi A, Nimura Y, Osada H, et al. Detailed characterization of a homozygously deleted region corresponding to a candidate tumor suppressor locus at 21q11-21 in human lung cancer. *Genes, chromosomes & cancer*. 2008 Sep; 47(9):810–818. [PubMed: 18523997]
37. Lu L, Katsaros D, de la Longrais IA, Sochirca O, Yu H. Hypermethylation of let-7a-3 in epithelial ovarian cancer is associated with low insulin-like growth factor-II expression and favorable prognosis. *Cancer research*. 2007 Nov 1; 67(21):10117–10122. [PubMed: 17974952]
38. Carrasco DR, Tonon G, Huang Y, Zhang Y, Sinha R, Feng B, et al. High-resolution genomic profiles define distinct clinico-pathogenetic subgroups of multiple myeloma patients. *Cancer Cell*. 2006 Apr; 9(4):313–325. [PubMed: 16616336]
39. Liang L, Wong CM, Ying Q, Fan DN, Huang S, Ding J, et al. MicroRNA-125b suppressed human liver cancer cell proliferation and metastasis by directly targeting oncogene LIN28B2. *Hepatology*. 2010 Nov; 52(5):1731–1740. [PubMed: 20827722]
40. Wang J, Cao N, Yuan M, Cui H, Tang Y, Qin L, et al. MicroRNA-125b/Lin28 pathway contributes to the mesendodermal fate decision of embryonic stem cells. *Stem Cells Dev*. 2012 Jun 10; 21(9):1524–1537. [PubMed: 22277001]
41. Rybak A, Fuchs H, Smirnova L, Brandt C, Pohl EE, Nitsch R, et al. A feedback loop comprising lin-28 and let-7 controls pre-let-7 maturation during neural stem-cell commitment. *Nat Cell Biol*. 2008 Aug; 10(8):987–993. [PubMed: 18604195]
42. Segalla S, Pivetti S, Todoerti K, Chudzik MA, Giuliani EC, Lazzaro F, et al. The ribonuclease DIS3 promotes let-7 miRNA maturation by degrading the pluripotency factor LIN28B mRNA. *Nucleic Acids Res*. 2015 May 26; 43(10):5182–5193. [PubMed: 25925570]
43. Lohr JG, Stojanov P, Carter SL, Cruz-Gordillo P, Lawrence MS, Auclair D, et al. Widespread genetic heterogeneity in multiple myeloma: implications for targeted therapy. *Cancer Cell*. 2014 Jan 13; 25(1):91–101. [PubMed: 24434212]
44. Bolli N, Avet-Loiseau H, Wedge DC, Van Loo P, Alexandrov LB, Martincorena I, et al. Heterogeneity of genomic evolution and mutational profiles in multiple myeloma. *Nature communications*. 2014; 5:2997.

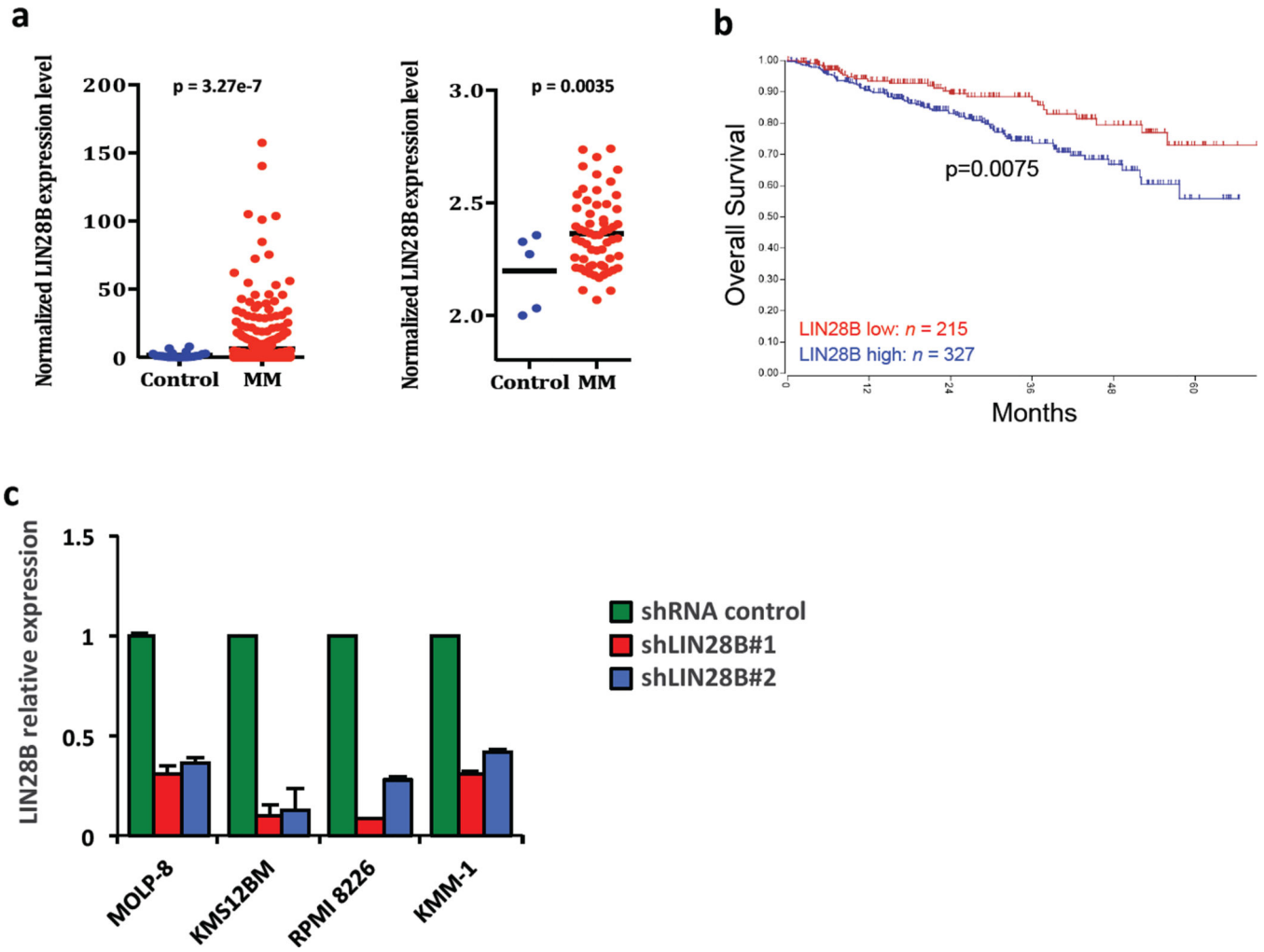


Figure 1. *LIN28B* expression level in MM
LIN28B expression level in MM patients, compared to healthy individuals, by analysis of (a) **Left panel:** GSE16558 (5 normal donor plasma cells and 65 plasma cell samples from patients with newly diagnosed MM) and **right panel:** GSE24080 – containing 22 normal donor plasma cell samples - and GSE2658 – 559 plasma cell samples from patients with newly diagnosed patients - both from UAMS, which were normalized using GeneSpring. (b) Kaplan-Meier analysis of 542 patients with MM of the Total Therapy 2 cohort (GSE2658). Patients were classified as high vs. low expression of *LIN28B* based on the mean expression level. *LIN28B* was associated with significantly worse overall survival, ($p=0.0075$). (c) MOLP-8, KMS12BM, RPMI 8226 and KMM-1 cells infected with control shRNA, or 2 different *LIN28B* shRNAs, were studied for relative expression of *LIN28B* mRNA as determined by qRT-PCR.

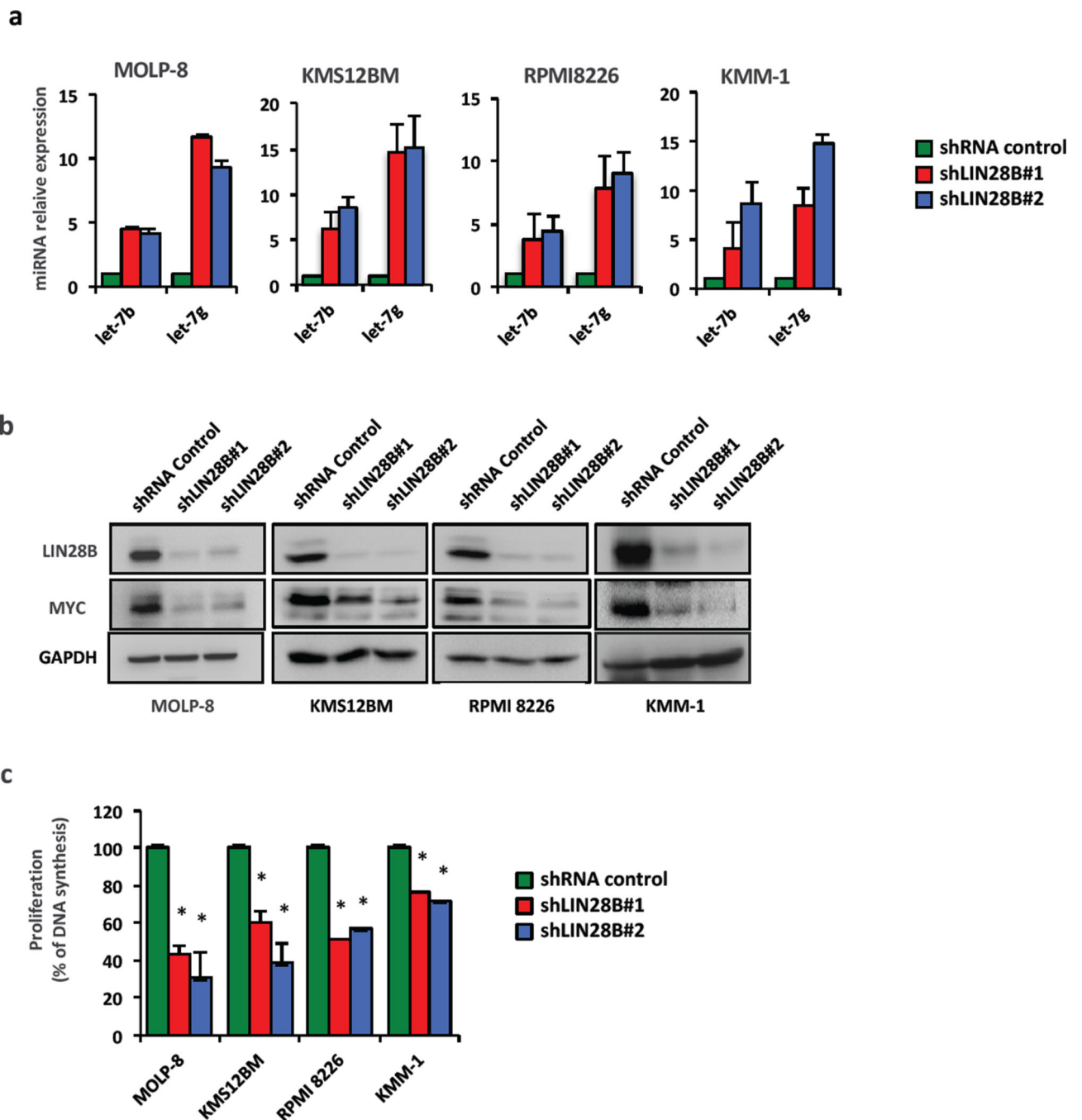


Figure 2. The *LIN28B*/*let-7*/*MYC* axis in Multiple Myeloma

(a) relative expression of mature *let-7* miRNA species as determined by quantitative PCR in 4 MM cell lines infected with control shRNA or 2 different *LIN28B* shRNAs. (b) Protein blot analysis for *LIN28B* and *MYC* expression in MOLP-8, KMS12BM, RPMI 8226 and KMM-1 cells infected with control shRNA or 2 different *LIN28B* shRNAs, and (c) proliferation assay by thymidine uptake over a 48hr time in the same cell lines. P values were obtained by two-tailed Student t test (* $P < 0.05$)

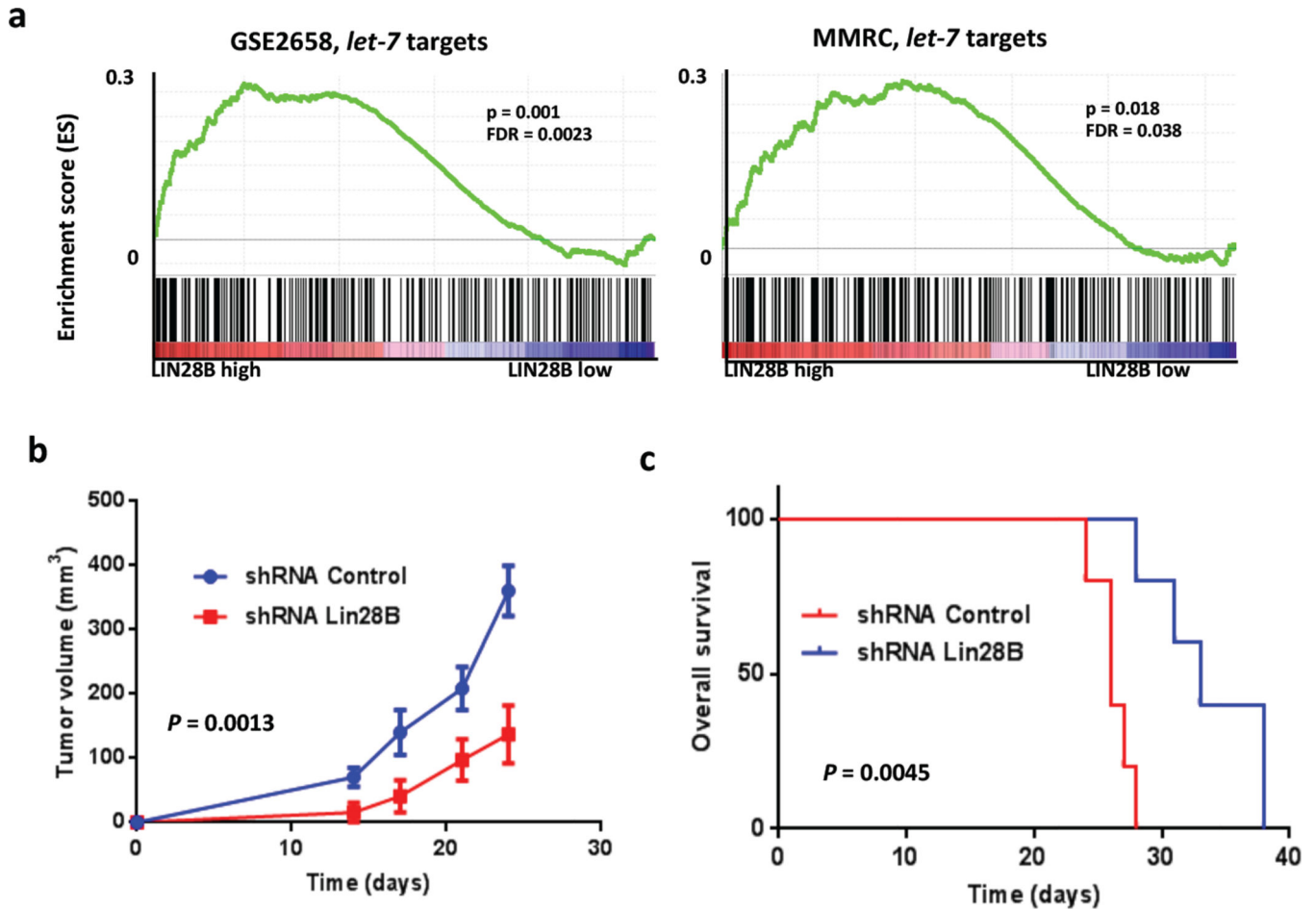


Figure 3. The *LIN28B/let-7* axis in data sets and in vivo

(a) GSEA analysis showing an enrichment of *let-7* target genes in MM patients who display a high level of *LIN28B* expression in two independent datasets (GSE2658 and MMRC dataset). (b) Tumor volume and (c) survival of SCID/bg mice (5 per group) injected subcutaneously with $5 \cdot 10^6$ MOLP-8 cells expressing pLKO control shRNA or pLKO.LIN28BshRNA; average survival time was 26 days versus 33 days, respectively, $P = 0.0045$. Bars indicate mean \pm SD ($n = 3$).

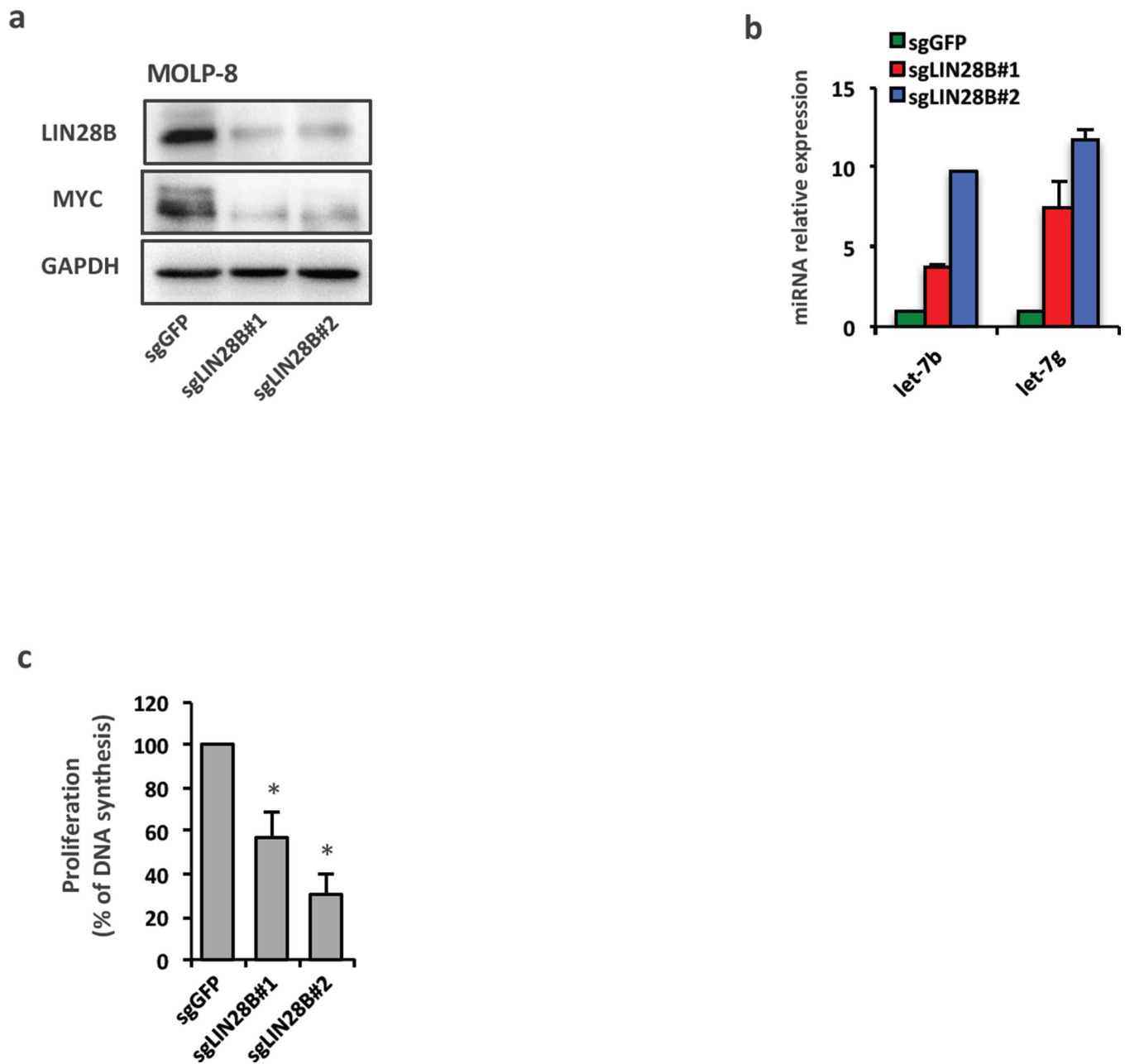


Figure 4. *LIN28B* KO with CRISPR/Cas9 leads to MYC regulation and *Let-7* upregulation
MOLP-8 cell line was infected with a lentiCRISPR control (sgGFP) or 2 different sgLIN28B and studied for (a) Protein blot analysis, (b) relative expression of *let-7* miRNAs by qRT-PCR and (c) proliferation assay by thymidine uptake. Bars indicate mean \pm SD (n = 3). P values were obtained by two-tailed Student t test (* $P < 0.01$).

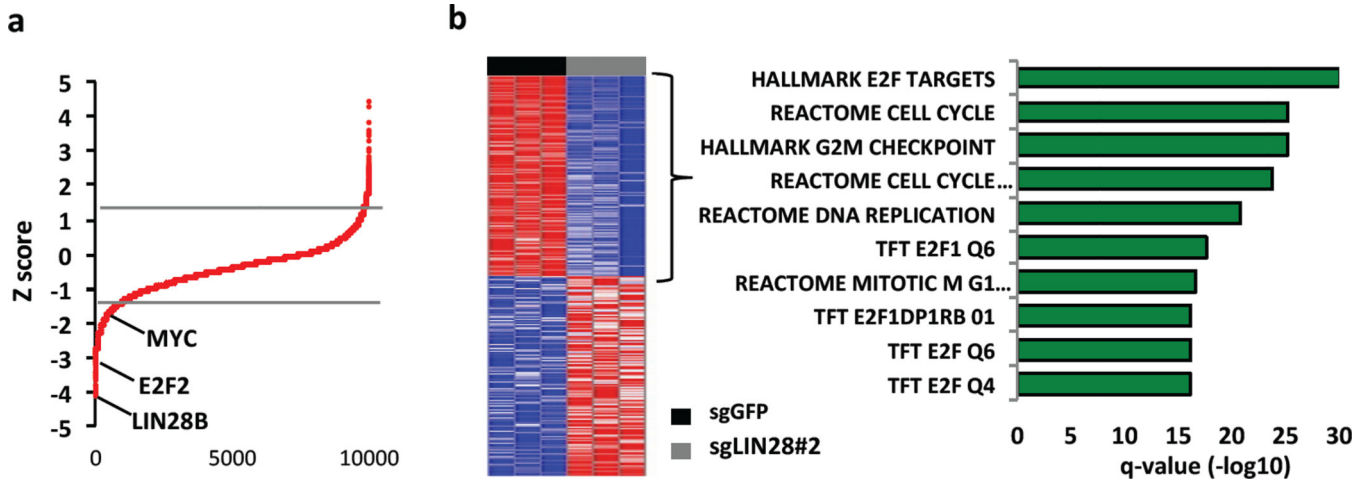


Figure 5. RNA sequencing and differential expression of genes downstream of *LIN28B*
 RNA sequencing was performed with MOLP-8 lentiCRISPR control and sgLIN28B#2. **(a)** Scatter plot showing differential expression of genes ranked by Z score (metric of fold change and $-\log_{10}$ of the p value) of control cells against *LIN28B*-silenced cells. **(b)** Heat map of the top 150 down-regulated and up-regulated genes in *LIN28B*-silenced cells. Bar plot representing the p value of the top 10 gene sets enriched in the high-*LIN28B* signature.

Author Manuscript

Author Manuscript

Author Manuscript

Author Manuscript

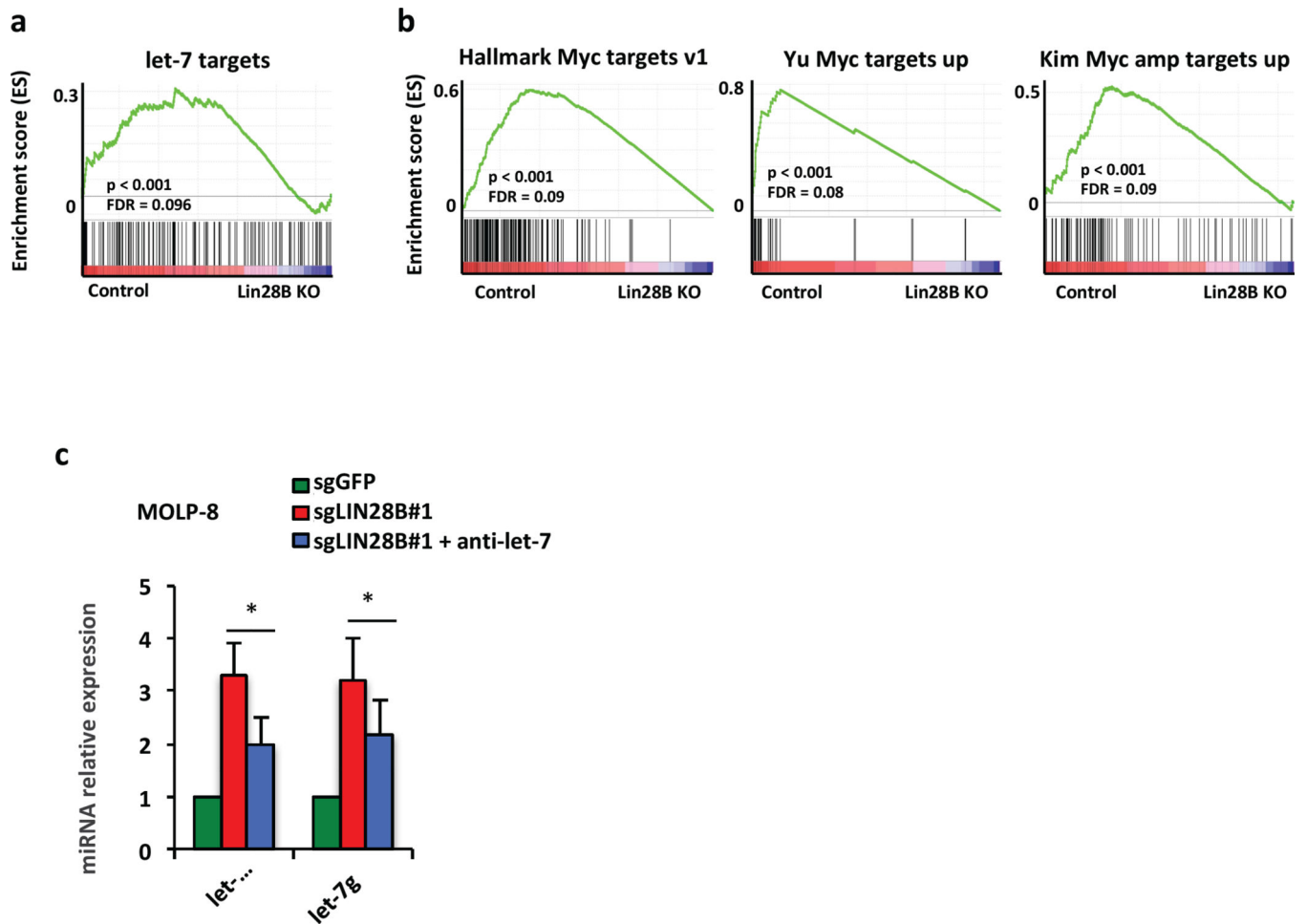


Figure 6. RNA sequencing and gene set enrichment analysis

(a) Gene set enrichment analysis (GSEA) for the *let-7* target gene set and (b) GSEA analysis for several *MYC* gene sets in control vs. *LIN28B* KO cells. (c) MOLP-8 cells were infected with either lentiCRISPR control (sgGFP) or sgLIN28B#1, and transfected with a control probe or a mix of anti-*let-7 b* and *g*. Cells were studied for *let-7* expression level by qRT-PCR.

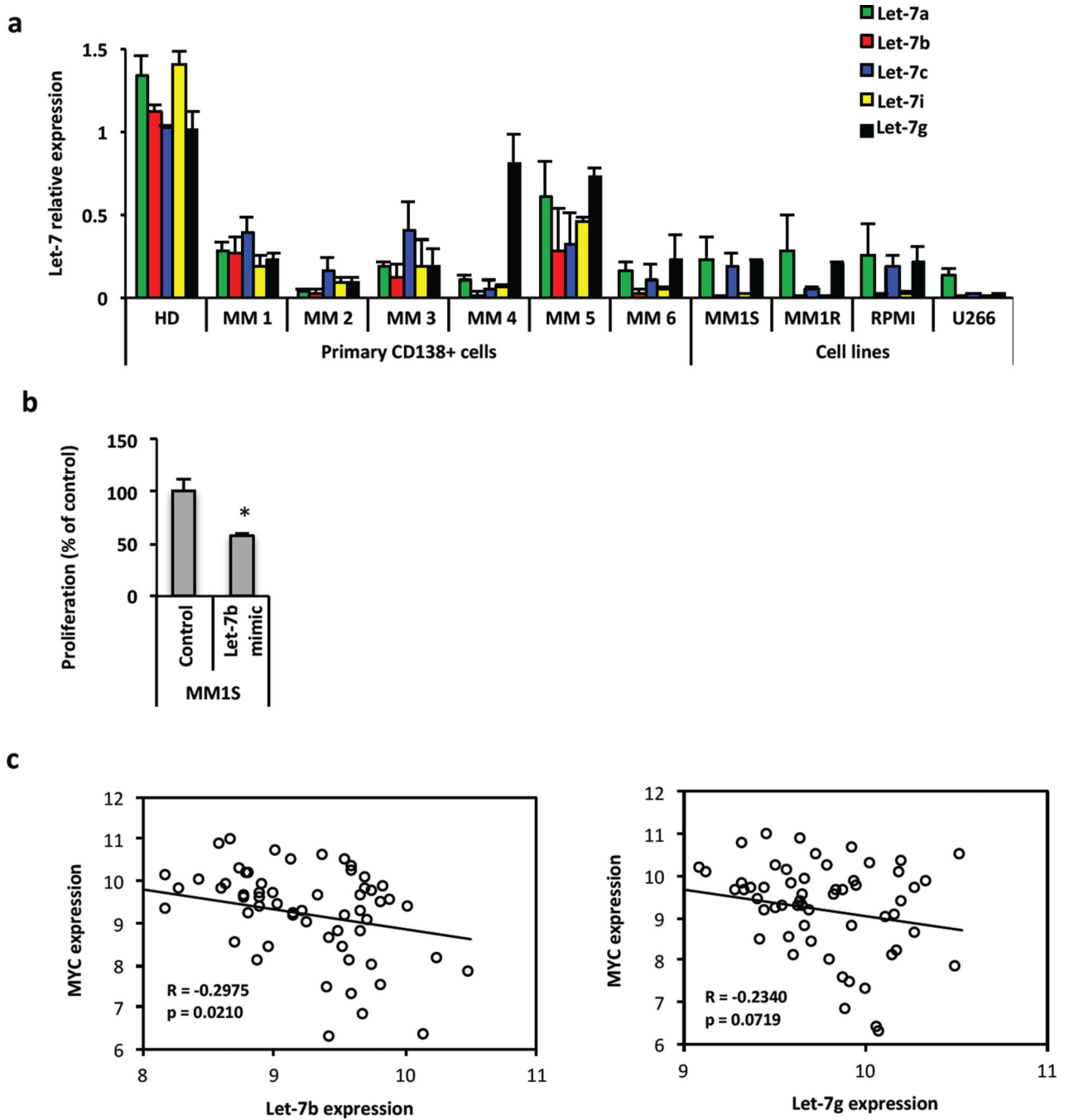


Figure 7. *Let-7* is down-regulated in MM and regulates *MYC*

(a) qRT-PCR analysis of *let-7* family members in primary plasma cells from healthy donors and MM patients, as well as in 4 MM cell lines. (b) proliferation assay using thymidine uptake and 72 hours after transfection of a *let-7b* mimic or a control probe in MM1S cells. Bars indicate mean \pm SD (n = 3). P values were obtained by two-tailed Student t test (* $P < 0.05$). (c) Correlation between *let-7* and *MYC* expression in patients with MM. Scatter plot showing the correlation between *let-7b* and *g*, respectively, and *MYC* from GSE16558. A Pearson correlation coefficient and a two-tailed p value were computed for each of them.

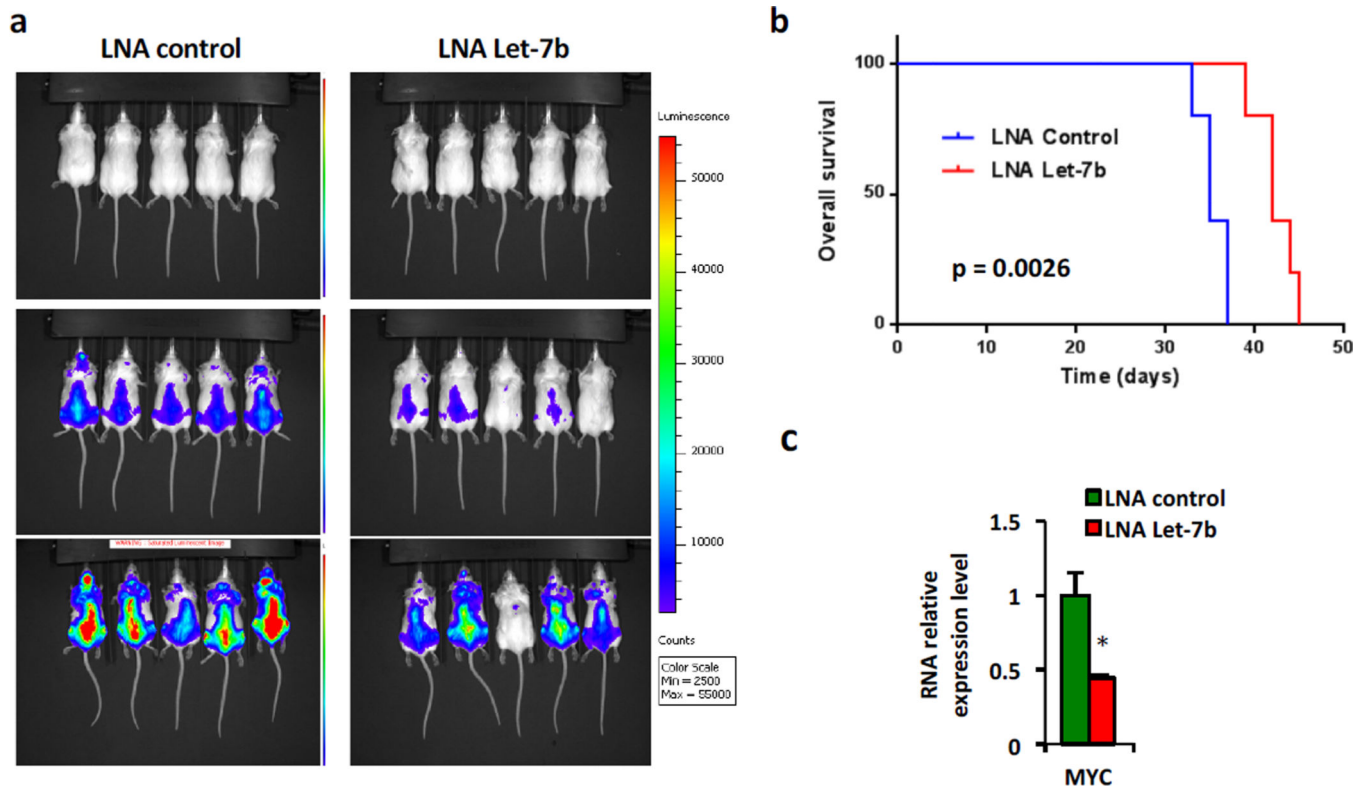


Figure 8. Increased expression of *let-7* in vivo decreases MM proliferation

(a) Mice were followed by bioluminescence intensity (BLI), after injection of 5 million of MM.1S GFP⁺Luc⁺ cells. SCID/bg mice (5 per group) were injected i.p. 2 times a week with 20mg/kg of LNA control or LNA *let-7* mimic. (b) Survival of the mice by Kaplan Meier analysis. Average survival time was 35 days in control group versus 42 days in LNA *let-7* mimic group, $P = 0.0026$. (c) qRT-PCR analysis of *MYC* in MM.1S cells *ex vivo*. Bars indicate mean \pm SD ($n = 3$). P values were obtained by two-tailed Student t test ($*P < 0.05$).